

THE EFFECT OF H₂ PURITY ON THE COMBUSTION, PERFORMANCE, EMISSIONS, AND ENERGY COSTS IN AN SPARK IGNITION ENGINE

by

Habib GURBUZ*

Department of Automotive Engineering, Faculty of Engineering,
Suleyman Demirel University, Isparta, Turkey

Original scientific paper
<https://doi.org/10.2298/TSCI180705315G>

This paper aims to examine the effect of hydrogen purity on the combustion, performance, NO_x emissions and energy costs in a spark ignition engine. In accordance with this purpose, two commercial hydrogen gases of different purity (i. e. 99.998% and 99.995%), were used as fuel in an spark ignition engine. The engine was operated under a lean mixture ($\phi = 0.6$) and wide-open throttle conditions at 1400, 1600, and 1800 rpm engine speeds. It was found that high purity hydrogen improves engine performance parameters (i. e. indicated power, torque, thermal efficiency, and specific fuel consumption) in the range of 2.4-1.9% depending on engine speed. The combustion duration and the cyclic variations were also decrease when the engine is operated with high purity hydrogen. However, NO_x emissions increase depending on engine speed in the range of 3.4-2.9% when high purity hydrogen is used as a fuel. In addition, energy costs with high purity H₂ increase in the range of 5.9-6.5% depending on engine speed.

Key words: *spark ignition engine, H₂ purity, combustion, engine performance, NO_x emission, energy costs*

Introduction

Fossil fuels such as coal, diesel, and gasoline are rapidly being consumed. Furthermore, these fuels are polluting the environment [1]. Moreover, governments have put into effect very strict environmental legislation to counter this, as well as protecting the fast depleting available fuel reserves. They have further supported research and the use of alternative fuels [2-4]. The alternative fuels such as biodiesel, natural gas, ethanol, dimethyl ether, and hydrogen in terms of energy security is topical subject for researchers in this field [5]. Hydrogen is the ideal candidate as an energy carrier for systems using energy while reducing adverse effects on our livable environment. Furthermore, hydrogen reduces dependence on imported petrol for countries without natural resources [6]. Hydrogen can be directly used in spark-ignition (SI) engines as a single fuel. Furthermore, hydrogen has a wide flammability range, so hydrogen engines can be operated on a very lean mixture with high thermal efficiency and low NO_x emissions [7]. Otherwise, the NO_x emissions increase after an equivalence ratio of 0.7 in a hydrogen SI engine [8]. The high-octane value of hydrogen allows the engine to operate at a high compression ratio, and thereby increases thermal efficiency [9]. In addition, the high diffusivity speed of hydrogen increases the mixing quality around cylinders, which increases the homogeneity of the in-cylinder charge [10]. Furthermore, hydrogen provides a complete combustion

*Author's, e-mail: habibgurbuz@sdu.edu.tr

process under very lean operation conditions, also permitting the engine to operate even in low load situations along with wide-open throttle (WOT) conditions [11]. The high adiabatic flame propagation speed of hydrogen can maintain stable combustion at a lean air-fuel mixture, allowing for a higher compression ratio by reducing the probability of knock and decrease cycle-by-cycle variations in the flame propagation period [12]. The lower ignition energy of hydrogen ensures engines are ignited in a lean mixture, resulting in allowing the hydrogen engine to operate at a wider range of excess air ratio [13]. The quenching distance of hydrogen is shorter than that of gasoline, which can lower hydrocarbon emissions [14]. However, the temperature required for auto ignition is considerably higher than that of conventional hydrocarbon fuels [15]. The NO_x are the only unwanted emissions of hydrogen combustion. The NO_x are the only contaminant component emissions of hydrogen engines. The induction technique of hydrogen plays a crucial role in determining the performance characteristics of the hydrogen engine [16]. Most hydrogen fueled SI engine research has focused on the port injection technique [11]. Port fuel injection offers higher engine efficiency, operation at more a leaner mixture, lower cyclic variation and lower NO_x emissions [17].

Hydrogen is accepted as a hopeful energy carrier due to its improved natural properties, such as a high energy density of 14.300 J/kgK, long-term viability, environmentally friendly combustion products, and production from various sources [18]. Hydrogen is not present in a free state throughout the universe, but is in abundance in compound form, otherwise, it could react quickly with other elements. Therefore, hydrogen can be obtained either from higher energy fossil fuels or lower energy water [19]. Hydrogen can be produced directly from fossil fuels using processes such as coal gasification, partial oxidation, thermal-cracking, and methane reforming. Furthermore, hydrogen can be produced by photo-biological processes, water thermolysis photo electrolysis or photolysis and dissociating water with electrolysis [20]. However, electrical energy is required for hydrogen production with water electrolysis. The use of electrical energy produced by burning fossil fuels in the electrolysis process of water for hydrogen production reduces total costs by 35% compared to the use of electricity generated in a hydroelectric plant [21]. The purification cost of hydrogen corresponds to 40-60% of the total cost of hydrogen production, depending on the production technology used. However, the produced hydrogen can be used as internal combustion engine fuel without subjecting it to any purification treatment. Therefore, the sale price of hydrogen produced is fairly competitive with the retail price of gasoline, especially in regions where required gasoline is imported [22].

This study presents the effect of hydrogen purity on combustion, engine performance, NO_x emissions and energy cost in a SI engine. Two commercial hydrogen gases of differing purity (*i. e.* 99.998% and 99.995%) were used as fuel in a SI engine. The hydrogen purity rate was compared in terms of its effect on combustion, cyclic variation, engine performance, exhaust emission, and energy cost. In this context, the paper reveals the relationship between increased NO_x emissions and energy costs despite improvements in engine performance parameters using high purity H₂.

Experimental set-up

Experimental studies were conducted on a single-cylinder L-head type SI engine with a cylinder volume of 476 cm³. The H₂ was injected into the intake manifold of the engine at a pressure of about 5 bar that is decreased using a pressure regulator from a 200 bar H₂ tank. The engine was operated with a WOT, under lean mixture ($\phi = 0.6$) an 8:1 compression ratio. Experimental studies were conducted at three different engine speeds (*i. e.* 1400, 1600, and 1800 rpm). The in-cylinder pressure was measured using a Kistler 6052C piezoelectric

pressure transducer and its charge amplifier (Kistler 5018A). The crank angle (CA) and TDC positions were encoded by using a shaft encoder (Kistler 2618B) producing 1800 pulses per revolution. The H₂ and air-flow rates were measured via Aalborg GFC67 and GFM77 types thermal mass-flow meters, with the equivalence ratio, ϕ , being calculated. The ignition timing and injection duration were controlled via an engine control unit (Motec-M4). The intake air temperature was maintained at a constant value of 30 °C using a peripheral interface controller temperature controller during the experimental studies. Inlet air pressure was measured using a Motec-M4 engine control unit and a manifold absolute pressure sensor during the experimental studies. The outlet shaft of the engine was coupled to a hydraulic dynamometer, and the engine speed was changed by varying the engine load. The probe of an emission analyzer (IMR 1400-C) was connected in a perpendicular position to the exhaust flow of the engine, and NO_x emissions, excess O₂ and exhaust gas temperature were measured. Figure 1 shows a schematic diagram of the experimental set-up.

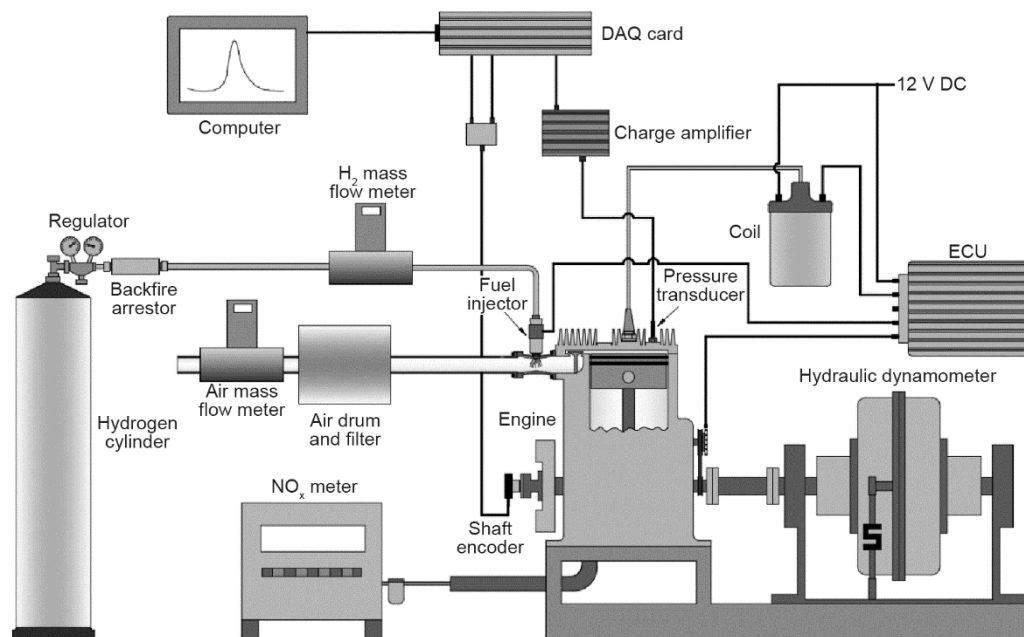


Figure 1. Schematic diagram of experimental set-up

A DAQ card (Measurement Computing-USB-1616HS-4) was connected to collect to the CA sensor and pressure transducer signals. The stored data on a PC computer was analyzed in order to calculate the engine and combustion parameters. For every working condition, 50 consecutive combustion cycles were operated in order to derive the corresponding *mean cycles* to the cylinder pressure data. The data obtained was used to calculate real time engine performance parameters, *i. e.* indicated thermal efficiency, η_i , indicated power, P_i , indicated torque, T_i , indicated specific fuel consumption, sfc_i , and combustion parameters, *i. e.* indicated mean effective pressure, $imep$, and mass fraction burned, mf_b .

The mf_b was calculated using an equation developed by Matekunas [23]. In the equation, the pressure ratio is defined as the ratio of the cylinder pressure from a firing cycle, $P(\theta)$, and the corresponding motored cylinder pressure, $P_o(\theta)$:

$$PR(\theta) = \frac{P(\theta)}{P_o(\theta)} - 1 \quad (1)$$

After this, the pressure ratio, PR , is normalized by its maximum value:

$$PR_N(\theta) = \frac{PR(\theta)}{PR(\theta)_{\max}} \quad (2)$$

In one paper in which the number of cycles was determined to calculate the cyclic variation, Gurbuz *et al.* [24] found that COV_{imep} increases linearly up to 50 consecutive combustion cycles and that there is an extremely small increase in COV_{imep} (3%) after 50 cycles. Therefore, the 50 consecutive combustion cycles were used to determine the cyclic variation in this paper. The cyclic variation of the combustion cycles was calculated from the in-cylinder pressure data using the coefficient of variation of $imep$ (COV_{imep}) as given in eq. (3) [25]:

$$COV_{imep} = \frac{\sigma_{imep}}{imep_{\text{mean}}} \times 100 \quad (3)$$

In this paper, two different commercial H₂ gases were used in industrial classification, defined as Hydrogen 4.6 (purity $\geq 99.996\%$) and Hydrogen 5.0 (purity $\geq 99.999\%$). In order to distinguish from between each hydrogen gas, Hydrogen 4.6 is defined as pure hydrogen and Hydrogen 5.0 is defined as high purity hydrogen. An elemental analysis of the commercial H₂ gas of two different purities used as engine fuel in this paper is given in tab. 1. The cost of the H₂ gas for Turkey is given in tab. 2.

Table 1. Commercial H₂ purity and other gas components

Component	Unit	High purity H ₂	Pure H ₂
H ₂	[%]	99.998	99.995
N ₂	[ppm]	13.097	29.778
O ₂	[ppm]	0.49	4.82
Moisture	[ppm]	1.7	5.43

Table 2. Cost of H₂ gas for Turkey

H ₂ purity	Tank water capacity [L]	Tank H ₂ pressure [bar]	Tank H ₂ capacity [m ³]	H ₂ cost (\$) + taxes for Turkey 8.2 m ³	H ₂ cost (\$) + taxes for Turkey [L]
High purity H ₂	50	200	8.2	197.986	0.0241
Pure H ₂	50	200	8.2	182.147	0.0222

Error analysis

An error analysis of the calculated (*i. e.* indicated power, indicated thermal efficiency, indicated specific fuel consumption, volumetric efficiency, and equivalence ratio,) and measured values (engine speed, in-cylinder pressure, CA, fuel-flow, air-flow NO_x, O₂, and exhaust gas temperature) was predicted using eq. (4).

$$\Delta R = \left[\left(\frac{\partial R}{\partial x_1} \Delta x_1 \right)^2 + \left(\frac{\partial R}{\partial x_2} \Delta x_2 \right)^2 + \dots + \left(\frac{\partial R}{\partial x_n} \Delta x_n \right)^2 \right]^{1/2} \quad (4)$$

The accuracy of the measurement equipment used in this paper is given in tab. 3. Error analysis of the measured parameters is given in tab. 4.

Table 3. Accuracy values of the measurement equipment

Variable	Device	Accuracy	
In-cylinder pressure	Kistler 6052C	±0.4% AR*	–
Crank angle	Kistler 2618B	±0.02°	–
Air-flow rate	Aalborg GFM77	±1.5% FS*	±0.48**
Hydrogen flow-rate	Aalborg GFC67	±1.5% FS*	±0.24**
Engine speed	Mag. Pick-up	±6 rpm AR*	–
Exhaust emission	IMR 1400 Compact	NO _x : ±80 ppm FS*	–
		O ₂ : ±0.2% FS*	–
		Temperature: ±1 °C FS*	–

*FS: Full scale, AR: All range **Accuracy of device in measurement range

Table 4. An error analysis of the measured and calculated parameters in this paper

Engine parameters	Calculated values at 1600 rpm	Error	Percentage [%]
P_i	2.813 kW	0.0159 kW	0.565
η_i	21.977%	0.142%	0.646
sfc_i	136.509 g/kWh	0.824 g/kWh	0.603
Volumetric efficiency	81.12%	0.608%	0.749
Equivalence ratio	0.6	0.0015	0.250
NO _x	1099 pp	10 ppm	0.910
O ₂	7.71%	0.028%	0.363
$T_{\text{exhaust gas}}$	364.8 °C	0.304 °C	0.835

Result and discussion

Figure 2 shows the variation of N₂, O₂, and moisture values vs. the H₂ purity rate for three different engine speeds. The components of the fuel gas (*i. e.* pure and high purity H₂) were calculated considering the amount of H₂ taken into the cylinder for each engine speed according to the data in tab. 1. The amount of moisture in the fuel is the most important factor affecting the flammability of the fuel. Moisture acts as a heat sink due to the evaporation of water, thus reducing the amount of oxygen in the combustion zone by diluting with flammability volatiles [26]. Under normal atmospheric conditions, nitrogen is an inert gas, and thus nitrogen is not significantly affected by the reaction [25]. Therefore, the nitrogen acts as a heat sink, such as moisture in the combustion reaction, and reduces the combustion temperature. In

other words, the combustion reaction is significantly influenced from by the amount of nitrogen. As a result of this, the increase in the amount of moisture and nitrogen in the fuel reduces the flammability of the fuel and causes a decrease in the engine performance parameters. It can be seen in fig. 2 that the N₂, O₂, and moisture increased 2.27, 9.46, and 3.19 times, respectively, with pure H₂ according to the high purity H₂. Generally, the increase in the amount of moisture and nitrogen in the pure H₂ significantly influenced the results of this paper (*i. e.* in-cylinder combustion, engine performance parameters, and exhaust NO_x emissions).

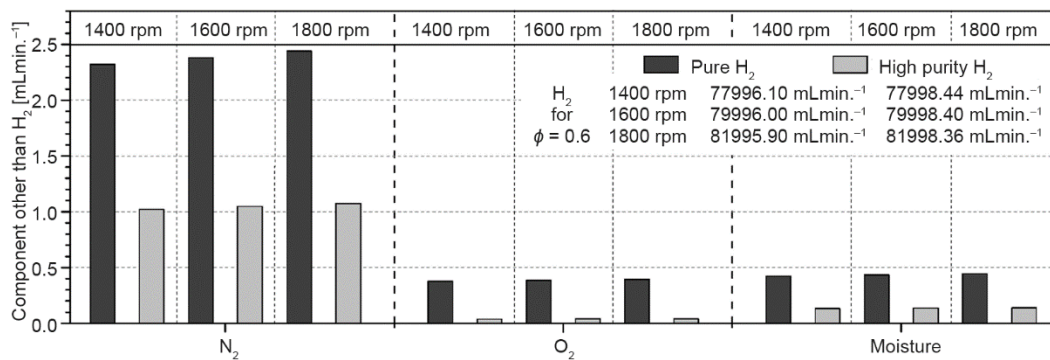


Figure 2. Variation of N₂, O₂, and moisture values vs. H₂ purity rate for the three engine speeds

The variation of *imep* vs. different SI timings for the three engine speeds is given in fig. 3. As shown in fig. 3, the *imep* increases at the optimum ignition timing minimum ignition advance for best torque (MBT) when the engine is operated with high purity H₂ for each of the three engine speeds. As shown in fig. 3, the mean effective pressure (*imep*) value at the MBT increases with the use of of high purity hydrogen for each of the three engine speeds. However, when the ignition timing was shifted from MBT timing to the retard ignition timing (TDC), the increase in the *imep* produced using high purity hydrogen is further increased. In contrast, when the ignition timing is shifted from MBT time to an expansion stroke (advance ignition timing), the increase in the *imep* produced using high purity hydrogen decreases, and the pure hydrogen become even more advantageous than the high purity hydrogen. This result is probably due to the fact that sufficient time for combustion, in the case of an over advanced position, compensates for the faster burning ability of high purity H₂. However, these conditions do not eliminate

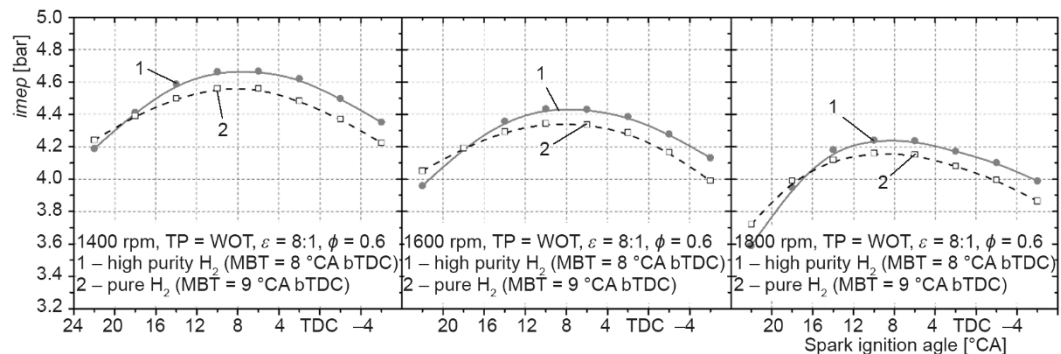


Figure 3. Variation of *imep* vs. different SI timings for three engine speeds

the positive effect of high purity H₂ at the MBT in terms of engine performance. However, the optimum ignition timing, corresponding to MBT, gets closer to TDC with high purity H₂. This effect is greater at low engine speeds (*i. e.* 1400 rpm), and even almost disappears at the high engine speeds (*i. e.* 1800 rpm). Following these results, MBT has been used in the investigation of combustion, engine performance, exhaust emission and energy costs in this paper.

Figure 4(a) illustrates the profiles of in-cylinder pressure *vs.* CA for three different engine speeds. In-cylinder pressure profiles were created by calculating the average of 50 consecutive combustion cycles. Engine speed increased with a reduction of engine output shaft load which caused a decrease of maximum pressure, P_{max} , for both H₂ purity rates, as shown in fig. 5. Furthermore, the combustion pressure curves split earlier from the motoring curve when the engine was operated with high purity H₂ for each of the three engine speeds. Furthermore, the position of P_{max} ($\phi_{P_{max}}$) got closer to TDC with high purity hydrogen for each of the three engine speeds. The P_{max} increased approximately in the range of 1.43-0.85 bar using high purity hydrogen, while engine speed changed between 1400-1600 rpm. The MBT ignition timing approached even closer to TDC with high purity hydrogen for each of the three engine speeds. Figure 4(b) shows the profiles of the in-cylinder pressure increase rate *vs.* CA for the three different engine speeds. Figure 4(b) shows the maximum rate of pressure rise (MRPR) raised when the engine was operated with high purity H₂. It can be seen that the MRPR decreased for both H₂ purity rates due to a reduction of in-cylinder pressure and temperature as a result of increasing engine speed. The increase in the MRPR was approximately 11.2%, 9.8%, and 7.4% at engine speeds of 1400, 1600, and 1800 rpm, respectively, when the engine was operated using high purity H₂. The highest MRPR was obtained at 1400 rpm, when the engine was operated with high purity H₂. However, this value is less than the 2.6 bar/°CA which is the knock limit of the SI engine.

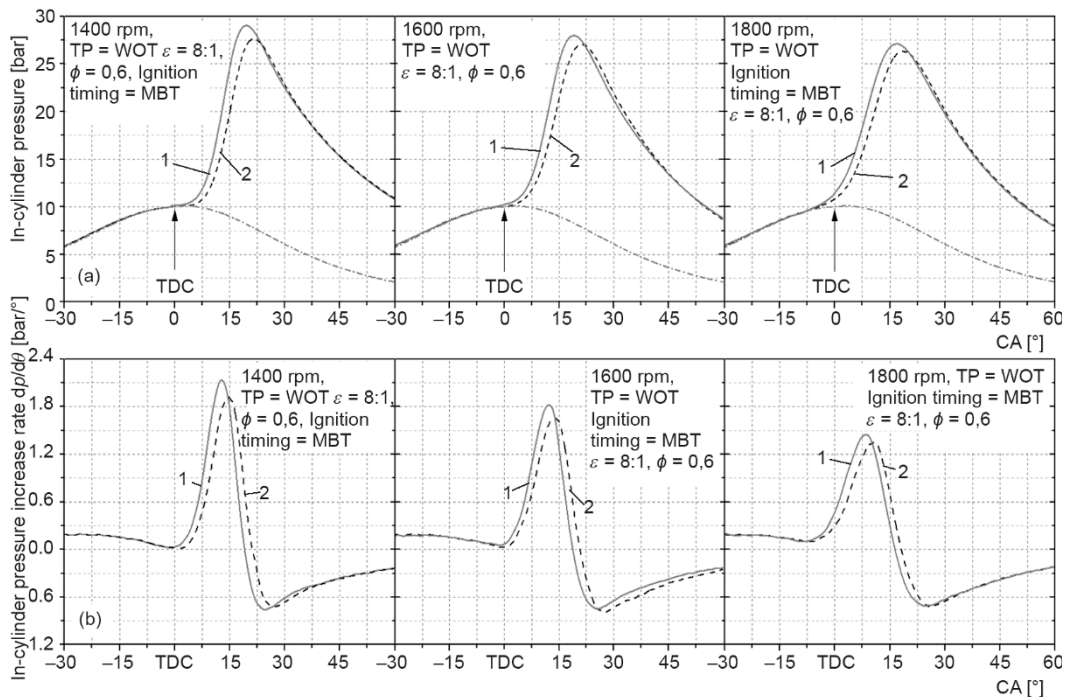


Figure 4. Variation of (a) cylinder pressure and (b) rate of pressure rise *vs.* H₂ purity for the three engine speeds; 1 – high purity H₂, 2 – pure H₂, 3 – motored pressure

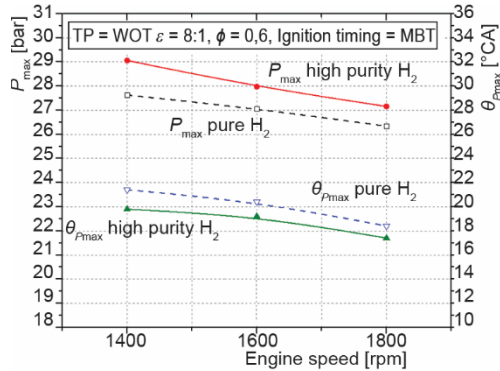


Figure 5. Variation of P_{\max} and $\theta_{P_{\max}}$ vs. H₂ purity for the three engine speeds

of the in-cylinder turbulence to the increase in combustion speed.

In-cylinder combustion in SI engines can be divided into three basic parts, defined depending on the CA, as the flame initiation period, the flame propagation period and the flame termination period [27]. Flame development and propagation duration are dealt with as two important factors influencing SI engine thermal efficiency [28]. The variation of *mfb* curves, according to the CA after ignition for the two H₂ purities at the three different engine speeds, is given in fig. 6. In addition to the CA positions for 0-10% *mfb*, 10-90% *mfb*, 100% *mfb* as well as 90% *mfb* are listed in tab. 5. In fig. 6, since the ignition timings corresponding to MBT for pure hydrogen and high purity hydrogen have changed, the *mfb* curves are given according to the normalized CA (CA after ignition). Therefore, it is possible to read the results given in tab. 5 through fig. 6. Figure 6 shows that the 0-10% *mfb* (flame initiation period), 10-90% *mfb* (flame propagation period), and 90-100% *mfb* shorten when high purity hydrogen is used as fuel. This shortening as the CA is higher in the flame initiation period than in the other two combustion periods, as shown in comparison to the burn angles given in tab. 5. The fast burning property of hydrogen increases with an increase in purity, and this effect becomes more dominant in the flame development angle, which is the slowest phase of combustion. The reduction in the total combustion duration is about 8.44%, 7.48%, and 6.20% at engine speeds of 1400, 1600, and 1800 rpm, respectively, when engine is operated with high purity H₂. The increase of engine speed causes an increase flame speed as a result of the increase in cylinder turbulence. The increased heat release rate, with the effect of high turbulence, causes an increase in *mfb*.

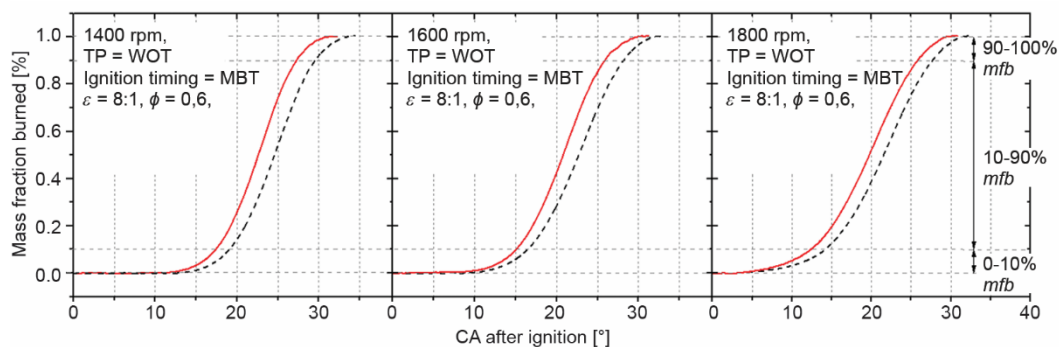


Figure 6. Variation of *mfb* vs. H₂ purity for different engine speeds; - - - pure H₂, — high purity H₂

The variation of P_{\max} and $\theta_{P_{\max}}$ vs. the H₂ purity for the three engine speeds is given in fig. 6. According to fig. 5, P_{\max} increased by approximately 5.2%, 3.4%, and 3.1% at engine speeds of 1400, 1600, and 1800 rpm, respectively, when the engine was operated with high purity H₂. Moreover, $\theta_{P_{\max}}$ decreased by about 8.1%, 6.3%, and 5.7% at engine speeds of 1400, 1600, and 1800 rpm, respectively, when operated with high purity H₂. These results appear as a result of an increased burning speed along with an increasing purity rate. The decrease in the effect on the pressure parameters of H₂ purity with engine speed, can be explained by the contribution of

Therefore, the effect of the hydrogen purity to the combustion duration is lower along with increased engine speeds. However, it is obvious that hydrogen purity contributes to the shortening of the combustion periods in addition to the increasing turbulence effect along with the increase in engine speed. Moreover, the effect of hydrogen purity on the flame termination period appears to be almost nonexistent. On the other hand, in-cylinder turbulence, which increases with engine speed, is also effective in the final flame period.

Table 5. The CA positions of combustion phase (mfb) vs. H₂ purity for the three engine speeds

Engine speed [rpm]	$\theta_i - \theta_{10}$ mfb			θ_{90} mfb		$\theta_{10} - \theta_{90}$ mfb			θ_{100} mfb		$\theta_{90} - \theta_{100}$ mfb			Difference in total combustion durations [%]
	H _{2-p} [°CA]	H _{2-tp} [°CA]	Difference [%]	H _{2-p} [°CA]	H _{2-tp} [°CA]	H _{2-p} [°CA]	H _{2-tp} [°CA]	Difference [%]	H _{2-p} [°CA]	H _{2-tp} [°CA]	H _{2-p} [°CA]	H _{2-tp} [°CA]	Difference [%]	
1400	19.0	17.4	10.34	29.4	27.2	10.4	9.8	6.12	33.4	30.8	3.8	3.6	5.5	% 8.44
1600	16.4	15.0	9.33	28.4	26.0	11.6	11.0	5.45	31.6	29.4	3.4	3.4		% 7.48
1800	13.8	12.6	9.52	27.6	25.8	13.8	13.2	4.54	30.8	29.0	3.2	3.2		% 6.20

Cyclic combustion variability is one of the main characteristics which affect the performance of SI engines. A cyclic variability above 10% significantly affects engine output power [24]. The variation of COV_{imep} vs. H₂ purity for the three engine speeds is given in fig. 7. In this paper, 50 consecutive combustion cycles are used while the COV_{imep} is calculated. It can be seen in fig. 7 that the COV_{imep} increases with increasing engine speed for both H₂ purities. However, COV_{imep} decreases with increasing H₂ purity for the three engine speeds. The reduction in COV_{imep} is approximately 6.5%, 4.2%, and 3.3% at engine speeds of 1400, 1600, and 1800 rpm, respectively, when the engine is operated with high purity H₂. This result shows that engine operation is more stable when operated with high purity hydrogen. As a result, we can say that stable engine operation contributes to the improvement of the engine performance parameters as given in fig. 8.

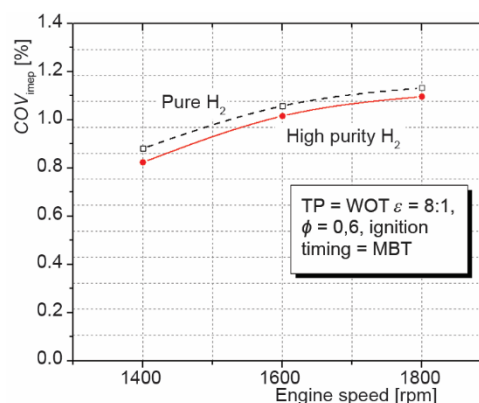


Figure 7. Variation of COV_{imep} vs. H₂ purity for three engine speeds

Figure 8 illustrates the variation of indicated power, P_i , indicated thermal efficiency, η_i , indicated torque, T_i , and indicated specific fuel consumption, sfc_i vs. H₂ purity for the three engine speeds. The P_i , η_i , and T_i increased with increasing H₂ purity, while sfc_i decreased. As can be seen in fig. 8, P_i , T_i , and η_i , owing to increasing H₂ purity, increased by approximately 2.4%, 2.1%, and 1.9% at engine speeds of 1400, 1600, and 1800 rpm, respectively, while $ISFC$ decreased at the same rates. The obtained improvement in the engine performance parameters using the high purity H₂, appeared as a result of the $imep$, which is increased by the effect of in-cylinder pressure and temperature.

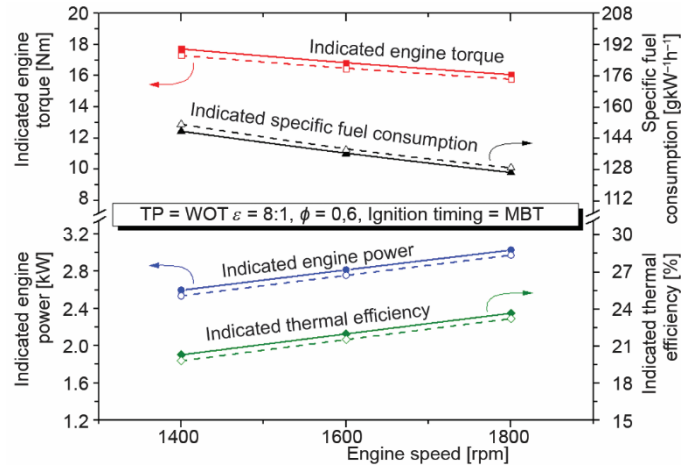


Figure 8. Variation of P_i , η_i , T_i , and sfc_i vs. H₂ purity for the three engine speeds; - - - pure H₂, — high purity H₂

The variation of exhaust NO_x emissions vs. H₂ purity for the three engine speeds is given in fig. 9(a). As a result of increasing engine speed, exhaust NO_x emissions decreased for both H₂ purity rates due to a reduction of in-cylinder pressure and temperature. As can be seen in fig. 9(a), exhaust NO_x emissions are increased about 3.4%, 3.1%, and 2.9% at engine speeds of 1400, 1600, and 1800 rpm, respectively, when the engine is operated with high purity H₂. On the other hand, the P_{max} is closer to TDC with high purity H₂ forming more time to recycle NO_x emissions in the expansion stroke. However, the cooling effect caused by the faster expansion causes the NO_x reactions to freeze and the concentration in the exhaust gases to increase. This effect can be seen from the shapes of the pressure curves in fig. 4. However, the amount of excess O₂ in the exhaust gases decreases due to the increase of NO_x emissions as shown in fig. 9(b). Moreover, the exhaust gas temperature changes very little with increasing H₂ purity, as shown in fig. 9(c). This is because, combustion slides towards the expansion stroke when the engine is operated with pure H₂, and the exhaust gas temperature increases slightly, as shown in fig. 9(c).

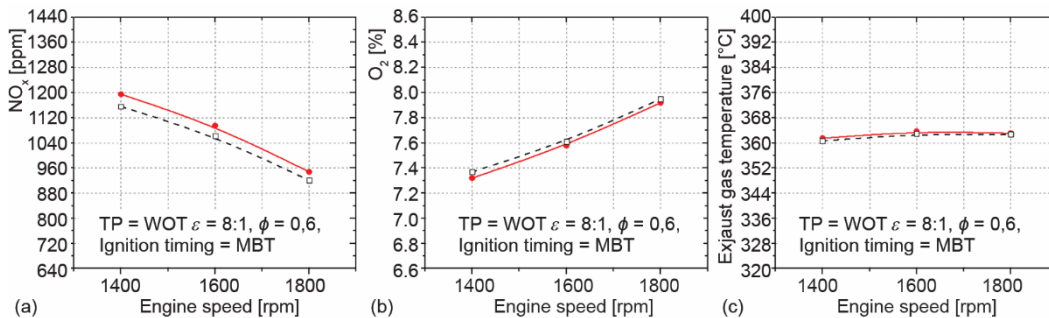


Figure 9. Variation of (a) NO_x, (b) O₂, and (c) exhaust gas temperature vs. H₂ purity for the three engine speeds; - - - pure H₂, — high purity H₂

Figure 10 shows the variation of energy costs vs. H₂ purity for the three engine speeds. The energy costs are calculated considering the generated indicated power against the amount of hydrogen taken into the cylinder for each engine speed. The energy costs increase by approximately 5.9%, 6.2%, and 6.5% at engine speeds of 1400, 1600, and 1800 rpm, respectively, when

the engine is operated with high purity hydrogen. It can be seen that the increasing energy costs and exhaust NO_x emissions, despite increasing engine power, lead to a reduction in overall system efficiency when the engine is operated with high purity hydrogen. However, high purity H₂ can be selected to increase the performance of the hydrogen engine, despite high exhaust emissions and energy costs. Furthermore, the price of hydrogen varies from country to country due to the influence of many factors (*i. e.* production and purification method of H₂, legal taxes, and shipping fees). Therefore, the results shown in fig. 10 may vary from country to country.

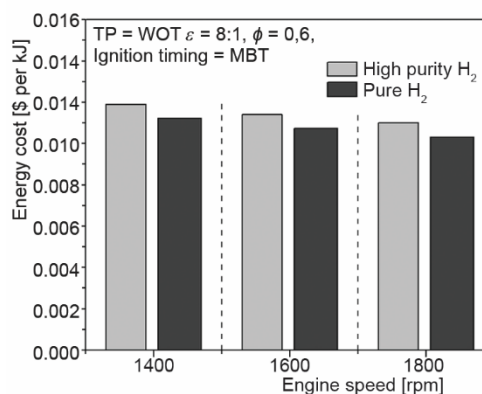


Figure 10. Variation of energy cost vs. H₂ purity for the three engine speeds

Conclusion

This paper seeks, at different engine speeds, to ascertain the effect of hydrogen purity on combustion, engine performance, NO_x emissions and energy costs in a SI engine. The conclusions of the study are as follows:

- The *imep* increased at the MBT with high purity H₂ for each the three engine speeds. Moreover, MBT came closer to TDC (towards retard position) with high purity H₂.
- The *P*_{max} increased approximately 5.2%, 3.4% and 3.1% at engine speeds of 1400, 1600, and 1800 rpm, respectively, when the engine is operated with high purity H₂. Moreover, *θ*_{*P*max} decreased about 8.1%, 6.3%, and 5.7% at engine speeds of 1400, 1600, and 1800 rpm, respectively, with high purity H₂.
- The total combustion duration decreased by approximately 8.44%, 7.48%, and 6.20% at engine speeds of 1400, 1600, and 1800 rpm, respectively, with high purity H₂. Moreover, the *COV*_{*imep*} decreased by approximately 6.5%, 4.2%, and 3.3% at engine speeds of 1400, 1600, and 1800 rpm, respectively, with high purity H₂.
- Engine performance parameters (*i. e.* indicated power, torque, thermal efficiency and specific fuel consumption) improved by approximately 2.4%, 2.1%, and 1.9% at engine speeds of 1400, 1600, and 1800 rpm, respectively, with high purity H₂.
- The NO_x emissions increased by approximately 3.4%, 3.1%, and 2.9% at engine speeds of 1400, 1600, and 1800 rpm, respectively, with high purity H₂. Moreover, the amount of excess O₂ in the exhaust gases decreased depending on increasing NO_x emissions.
- As a general result, the increase in the amount of moisture and nitrogen in the pure H₂ according to the high purity H₂, negatively influenced the results of this paper (*i. e.* in-cylinder combustion, engine performance parameters and exhaust NO_x emissions).
- Furthermore, the energy costs increased by approximately 5.9%, 6.2%, and 6.5% at engine speeds of 1400, 1600, and 1800 rpm, respectively, with high purity H₂. However, it can be said that high purity H₂ as a fuel can be preferred to increase the performance of the hydrogen engine, despite high exhaust emissions and energy costs.

Nomenclature

*COV*_{*imep*} – coefficient of variations of *imep*
 H_{2-p} – pure hydrogen
 H_{2-hp} – high purity hydrogen

imep – indicated mean effective pressure, [bar]
*imep*_{mean} – mean value of *imep*, [bar]

m_{fb}	– mass fraction burned [%]
P	– in-cylinder pressure, [bar]
P_i	– indicated power, [kW]
P_{max}	– maximum pressure, [bar]
P_o	– motored cylinder pressure, [bar]
PR	– pressure ratio, [bar]
sfc_i	– indicated specific fuel consumption, [gkW ⁻¹ h ⁻¹]
$T_{exhaust\ gas}$	– exhaust gas temperature, [°CA]
T_i	– indicated torque, [Nm]
0-10% m_{fb}	– flame initiation period, [°CA]
10-90% m_{fb}	– flame propagation period, [°CA]
90-100% m_{fb}	– flame termination period, [°CA]

Greek symbols

ε	– compression ratio
η_i	– indicated thermal efficiency, [%]
θ	– instant crank angle, [degrees]
σ_{imep}	– standard deviation of imep
ϕ	– lean mixture
$\phi_{P_{max}}$	– position of P_{max} , [°CA]

Acronyms

MBT	– maximum brake torque, [Nm]
MRPR	– maximum rate of pressure rise
ppm	– particle per million
TP	– throttle position
WOT	– wide-open throttle

References

- [1] Alazemi, J., Andrews, J., Automotive Hydrogen Fueling Stations: An International Review, *Renew. Sustain. Energy Rev.*, 48 (2015), Aug., pp. 483-499
- [2] Ganesh, R. H., *et al.*, Hydrogen Fueled Spark Ignition Engine with Electronically Controlled Manifold Injection: An Experimental Study, *Renewable Energy*, 33 (2008), 6, pp. 1324-1333
- [3] Verhelst, S., *et al.*, A Comprehensive Overview of Hydrogen Engine Design Features, *J. Automobile*, 221 (2005), 8, pp. 911-920
- [4] Balat, M., Potential Importance of Hydrogen as a Future Solution to Environmental and Transportation Problems, *Int. J. Hydrogen Energy*, 33 (2008), 15, pp. 4013-4029
- [5] Korakiznitis, T., *et al.*, Natural-Gas Fueled Spark Ignition (SI) and Compression-Ignition (CI) Engine Performance and Emissions, *Prog. Energy Combust. Sci.*, 37 (2011), 1, pp. 89-112
- [6] Sakintunaa, B., *et al.*, Metal Hydride Materials for Solid Hydrogen Storage: A Review, *Int. J. Hydrogen Energy*, 32 (2007), 9, pp. 1121-1140
- [7] Ghazal, O. H., Performance and Combustion Characteristic of CI Engine Fueled with Hydrogen Enriched Diesel, *Int. J. Hydrogen Energy*, 38 (2013), 35, pp. 15469-15476
- [8] Sakthinathan, G. P., Jeyachandran, K., Theoretical and Experimental Validation of Hydrogen Fueled Spark Ignition Engine, *Thermal Science*, 14 (2010), 4, pp. 989-1000
- [9] Ji, C., *et al.*, Effect of Spark Timing on the Performance of a Hybrid Hydrogen–Gasoline Engine at Lean Conditions, *Int. J. Hydrogen Energy*, 35 (2010), 5, pp. 2203-2212
- [10] Salvi, B. L., Subramanian, K. A., Sustainable Development of Road Transportation Sector Using Hydrogen Energy System, *Renew. Sustain. Energy Rev.*, 51 (2015), Nov., pp. 1132-1155
- [11] White, C. M., *et al.*, The Hydrogen-Fueled Internal Combustion Engine: A Technical Review, *Int. J. Hydrogen Energy*, 31 (2006), 10, pp. 1292-1305
- [12] Ma, F., *et al.*, Effects of Hydrogen Addition on Cycle-by-Cycle Variations in a Lean Burn Natural Gas Spark-Ignition Engine., *Int. J. Hydrogen Energy*, 2 (2008), 2, pp. 823-831
- [13] Shivaprasad, K. V., *et al.*, Experimental Investigation of the Effect of Hydrogen Addition on Combustion Performance and Emissions Characteristics of a Spark Ignition High Speed Gasoline Engine, *Procedia Technology*, 14 (2014), 1, pp. 141-148
- [14] Ceper, B. A., *et al.*, Investigation of Cylinder Pressure for H₂/CH₄ Mixtures at Different Loads, *Int. J. Hydrogen Energy*, 34 (2009), 11, pp. 4855-4861
- [15] Antunes, J. M. G., *et al.*, An Investigation of Hydrogen-Fuelled HCCI Engine Performance and Operation, *Int. J. Hydrogen Energy*, 33 (2008), 20, pp. 5823-5828
- [16] Suwanchotchoung, N., Performance of a Spark Ignition Dual-fuelled Engine Using Split Injection Timing, Ph. D. thesis, Mechanical Engineering, Vanderbilt University, Nashville, Tenn., USA, 2003
- [17] Yi, H. S., *et al.*, The Optimized Mixture Formation for Hydrogen Fuelled Engines, *Int. J. Hydrogen Energy*, 25 (2000), 7, pp. 685-690
- [18] Cipriani, G., *et al.*, Perspective on Hydrogen Energy Carrier and its Automotive Applications, *Int. J. Hydrogen Energy*, 39 (2014), 16, pp. 8482-8494
- [19] Verhelst, S., Recent Progress in the Use of Hydrogen as a Fuel for Internal Combustion Engines, *Int. J. Hydrogen Energy*, 39 (2014), 2, pp. 1071-1085

- [20] Alazemi J., Andrews J., Automotive Hydrogen Fuelling Stations: An International Review., *Renew. Sustain. Energy Rev.*, 48 (2015), Aug., pp. 483-499
- [21] Steinberg, M., Cheng, H. C., Modern and Prospective Technologies for Hydrogen Production from Fossil Fuels, *Int. J. Hydrogen Energy*, 14 (1989), 11, pp. 797-803
- [22] Gambini, M., Vellini, M., Comparative Analysis of H₂/O₂ Cycle Power Plants Based on Different Hydrogen Production Systems from Fossil Fuels, *Int. J. Hydrogen Energy*, 30 (2005), 6, pp. 593-604
- [23] Matekunas, F., Modes and Measures of Cyclic Combustion Variability, SAE Technical Paper 830337, 1983
- [24] Gurbuz, H., *et al.*, An Investigation on Effect of In-Cylinder Swirl Flow on Performance, Combustion and Cyclic Variations in Hydrogen Fuelled Spark Ignition Engine, *Journal of the Energy Institute*, 87 (2014), 1, pp. 1-10
- [25] Heywood, J. B., *Internal Combustion Engine Fundamentals*, McGraw-Hill, London, 1988
- [26] Shafizadeh, F., *et al.*, Effective Heat Content of Green Forest Fuels, *For. Sci.*, 23 (1977), 1, pp. 81-89
- [27] Kang, K. Y., Reitz, R. D., The Effect of Intake Valve Alignment on Swirl Generation in a DI Diesel Engine, *Exp. Therm. Fluids Sci.*, 20 (1999), 2, pp. 94-103
- [28] Syred, N., A Review of Oscillation Mechanisms and the Role of the PVC in Swirl Combustion Systems, *Prog. Energy Combust Sci.*, 32 (2006), 2, pp. 93-161